Am J Physiol Lung Cell Mol Physiol 312: L268–L276, 2017.
First published December 21, 2016; doi:10.1152/ajplung.00151.2016.

RESEARCH ARTICLE

A keratan sulfate disaccharide prevents inflammation and the progression of emphysema in murine models

Congxiao Gao,[1]* Reiko Fujinawa,[1]* Takayuki Yoshida,[2] Manabu Ueno,[3] Fumi Ota,[1] Yasuhiko Kizuka,[1] Tetsuya Hirayama,[4] Hiroaki Korekane,[1] Shinobu Kitazume,[1] Toshitaka Maeno,[3] Kazuaki Ohtsubo,[1,5] Keiichi Yoshida,[1] Yoshiki Yamaguchi,[1] Bernd Lepenies,[6] Jonas Aretz,[7,8] Christoph Rademacher,[7,8] Hiroki Kabata,[9] Ahmed E. Hegab,[9] Peter H. Seeberger,[7,8] Tomoko Betsuyaku,[9] Kozui Kida,[10] and Naoyuki Taniguchi[1]

[1]*Systems Glycobiology Research Group, RIKEN-Max Planck Joint Research Center for Systems Chemical Biology, Global Research Cluster, Hirosawa, Wako, Saitama, Japan;* [2]*First Department of Medicine, Hokkaido University School of Medicine, Sapporo, Hokkaido, Japan;* [3]*Department of Medicine and Biological Science, Gunma University Graduate School of Medicine, Gunma, Japan;* [4]*Central Research Laboratories, Seikagaku Corporation, Higashiyamato, Tokyo, Japan;* [5]*Faculty of Life Sciences, Kumamoto University, Kumamoto, Japan;* [6]*University of Veterinary Medicine Hannover, Research Center for Emerging Infections and Zoonoses, Infection Immunology, Hannover, Germany;* [7]*Department of Biomolecular Systems, Max Planck Institute of Colloids and Interfaces, Potsdam, Germany;* [8]*Department of Biology, Chemistry and Pharmacy, Freie Universität Berlin, Berlin, Germany;* [9]*Division of Pulmonary Medicine, Department of Medicine, Keio University, School of Medicine, Tokyo, Japan; and* [10]*Respiratory Care Clinic, Nippon Medical School, Tokyo, Japan*

Submitted 14 April 2016; accepted in final form 15 December 2016

Gao C, Fujinawa R, Yoshida T, Ueno M, Ota F, Kizuka Y, Hirayama T, Korekane H, Kitazume S, Maeno T, Ohtsubo K, Yoshida K, Yamaguchi Y, Lepenies B, Aretz J, Rademacher C, Kabata H, Hegab AE, Seeberger PH, Betsuyaku T, Kida K, Taniguchi N. A keratan sulfate disaccharide prevents inflammation and the progression of emphysema in murine models. *Am J Physiol Lung Cell Mol Physiol* 312: L268–L276, 2017. First published December 21, 2016; doi:10.1152/ajplung.00151.2016.—Emphysema is a typical component of chronic obstructive pulmonary disease (COPD), a progressive and inflammatory airway disease. However, no effective treatment currently exists. Here, we show that keratan sulfate (KS), one of the major glycosaminoglycans produced in the small airway, decreased in lungs of cigarette smoke-exposed mice. To confirm the protective effect of KS in the small airway, a disaccharide repeating unit of KS designated L4 ([SO_3^--6]Galβ1–4[SO_3^--6]GlcNAc) was administered to two murine models: elastase-induced-emphysema and LPS-induced exacerbation of a cigarette smoke-induced emphysema. Histological and microcomputed tomography analyses revealed that, in the mouse elastase-induced emphysema model, administration of L4 attenuated alveolar destruction. Treatment with L4 significantly reduced neutrophil influx, as well as the levels of inflammatory cytokines, tissue-degrading enzymes (matrix metalloproteinases), and myeloperoxidase in bronchoalveolar lavage fluid, suggesting that L4 suppressed inflammation in the lung. L4 consistently blocked the chemotactic migration of neutrophils in vitro. Moreover, in the case of the exacerbation model, L4 inhibited inflammatory cell accumulation to the same extent as that of dexamethasone. Taken together, L4 represents one of the potential glycan-based drugs for the treatment of COPD through its inhibitory action against inflammation.

chronic obstructive pulmonary disease; glycan; keratan sulfate; L4

CHRONIC OBSTRUCTIVE PULMONARY DISEASE (COPD), a disease characterized by irreversible airflow obstruction and alveolar destruction (23), is now a major worldwide health problem in terms of associated morbidity and mortality (24). COPD patients are more likely to develop a greater degree of inflammation in their airways due to bacterial or viral infections and air pollutants (11). Some phenotypes of COPD cause some patients to have frequent COPD episodes, resulting in a rapid deterioration in lung function and poor outcomes. These episodes of COPD are accompanied by extensive pathological changes to the lung. Inflammation, particularly of the small airways, is characterized by an accumulation of inflammatory cells, such as neutrophils, macrophages, and dendritic cells (2). These cells, along with airway epithelial cells, release reactive oxygen species, cytokines, chemokines, elastase, and matrix metalloproteinases (MMPs) that are responsible for the pathogenesis of COPD (2). Although pharmacology therapy is employed to control these symptoms, there is a pressing need to develop novel approaches for preventing the progression of airflow limitations and/or emphysema (11).

Glycans, which are functionally attached to various biomolecules, including proteins and lipids, play important roles in the interaction of cells with the surrounding extracellular matrix, which is important in a variety of physiological and pathological phenomena, including inflammation. In our previous studies, $\alpha_{1,6}$-fucosyltransferase (FUT8), a glycosylation enzyme that catalyzes the biosynthesis of a core fucose structure in *N*-glycans, was purified to homogeneity, and its cDNA was cloned (30). We found that *Fut8*-null mice developed emphysematous changes (32) and that a reduced level of core fucose results in an elevated sensitivity to cigarette smoke-induced emphysema in mice (8). FUT8 levels are also related to the

* C. Gao and R. Fujinawa contributed equally to this article.
Address for reprint requests and other correspondence: N. Taniguchi, Systems Glycobiology Research Group, RIKEN-Max Planck Joint Research Center for Systems Chemical Biology, Global Research Cluster, RIKEN, 2-1 Hirosawa, Wako, Saitama, 351-0198, Japan (e-mail: dglycotani@riken.jp).

outcome of human COPD patients, namely, the frequency of exacerbations and the decline of lung function, which are typical of COPD patients (16). Moreover, endogenous glycosaminoglycans (GAGs), including keratan sulfate (KS), hyaluronan, chondroitin sulfate/dermatan sulfate, and heparan sulfate/heparin, are expressed in the interstitium, the subepithelial tissue, the bronchial walls, and in airway secretions (20). GAGs play important roles in numerous biological functions, such as controlling growth, signal transduction, and cell adhesion (31). KS has been shown to inhibit the expression and activation of MMP-2 in corneal and skin explant cultures (13), suggesting that it may have protective effects from tissue damage. We recently reported that a KS disaccharide, L4 ([SO_3^--6]Galβ1–4[SO_3^--6]GlcNAc), specifically blocked the interaction of bacterial flagellin with Toll-like receptor 5 and subsequently suppressed the production of IL-8 in normal human bronchial epithelial (NHBE) cells (27). In addition, L4 was also reported to suppress the production of IL-12 in macrophages that had been stimulated with LPS (33). The fact that KS is located at the apical border of NHBE cells and on the apical surface of ciliated cells in human tracheal tissue sections (20) suggests that it could be one of the substances that interact with inflammatory cells at an early stage in the process of inflammation.

Here, we report that L4 protects the lung from destruction by reducing the influx of inflammatory cells and decreasing the levels of inflammatory cytokines and MMPs, in the inflammatory process of emphysema or its exacerbation model in mice.

MATERIALS AND METHODS

Materials. LPS-free L4, [SO_3^--6]Galβ1–4[SO_3^--6]GlcNAc, was isolated from the digest of KS from shark fins with keratanase II, as previously described (33). Porcine pancreatic elastase (PPE) was obtained from Wako (Osaka, Japan). Other reagents and chemicals were obtained from commercial sources as indicated.

Cell cultures. The murine macrophage cell line RAW 264.7 was purchased from American Type Culture Collection (Manassas, VA) and cultured in DMEM (Sigma-Aldrich, St. Louis, MO), supplemented with 10% heat-inactivated FBS, 50 U/ml penicillin, and 50 μg/ml streptomycin (Nacalai, Kyoto, Japan). The cultures were maintained at 37°C in a humidified incubator containing 5% CO_2.

Mice. C57BL/6J mice were purchased from Oriental Yeast (Tokyo, Japan). The mice were housed under a 12:12-h light-dark cycle, fed standard chow, and given free access to food and water. All experimental protocols and procedures were approved by the Ethical Committee on Animal Research of the Hokkaido University School of Medicine and were performed in compliance with the Institutional Guidelines for Animal Experiments of RIKEN.

PPE-induced emphysema model. PPE (5 U; Wako), dissolved in 100 μl of sterile PBS or PBS alone, was sprayed into the tracheas of each mouse using a MicroSprayer drug delivery device (Penn-Century, Philadelphia, PA), as described previously (28).

Cigarette smoke exposure and LPS-induced exacerbation model. Cigarette smoke exposure was performed on $\alpha_{1,6}$-fucosyltransferase (*Fut8*) heterozygous mice (32) using two unfiltered Kentucky cigarettes per day, 6 days per week for 3 mo, as described previously (8). LPS was administered after the completion of the cigarette smoke exposure. LPS (1 mg/kg) (Sigma-Aldrich), dissolved in 100 μl of PBS, was sprayed into the tracheas of each mouse using the MicroSprayer drug delivery device.

mRNA extraction, reverse transcription, and real-time PCR. Total RNAs were extracted from mouse lungs using TRIzol (Thermo Fisher Scientific, Waltham, MA) and then purified using an RNeasy micro kit (Qiagen, Hilden, Germany), according to the manufacturers' protocols. Total RNA (0.5 μg) was reverse-transcribed using a SuperScript III First-Strand Synthesis System (Thermo Fisher Scientific). For real-time PCR, cDNA was mixed with Thunderbird SYBR qPCR Mix (Toyobo, Osaka, Japan) and amplified using an ABI PRISM 7900HT. The levels of *Chst1* and *Chst5* mRNAs were normalized to the corresponding levels of *Rpl4*. Primers for *Chst1*, *Chst2*, and *Chst5* were purchased from Qiagen (Mm_Chst1_1_SG, Mm_Chst2_1_SG and Mm_Chst5_1_SG). Primers for *Rpl4* were 5′-GTTCAAAGCTCCCATTCGAC-3′ and 5′-AATTCACTGACGGCATAGGG-3′.

Tissue preparation and histological analysis. On completion of the experimental protocol, mice were euthanized by CO_2 inhalation. Lungs were inflated by instilling 10% formalin at a constant pressure of 25 cm H_2O for 10 min, and the inflated lungs were fixed for 24 h. Serial midsagittal sections were obtained for morphological and histological analyses.

After fixation, the paraffin-embedded tissues were sectioned (5 μm) and stained with hematoxylin and eosin. Mean linear intercepts (L_m) were calculated on the basis of 20 randomly selected fields in each section at ×100 magnification with two crossed test lines (18).

Mouse anti-KS (5D4) (Seikagaku, Tokyo, Japan), rabbit anti-aquaporin-5 (Abcam, Cambridge, UK), and rabbit anti-surfactant protein-C (Merck-Millipore, Darmstadt, Germany) antibodies were used in immunofluorescence staining, as described previously (9). DAPI was added to stain nuclei.

L4 administration. To assess the anti-inflammatory effect of L4, L4 (250 μg/body) suspended in 50 μl of saline or 50 μl of saline alone was intravenously administrated at 0.5 h before intratracheal PPE treatment. The mice were euthanized by CO_2 narcosis at 24 h after PPE treatment, and tissue sampling was performed. For the suppressive effects of L4 on air space enlargement due to PPE treatment, L4 was administered intravenously on two further occasions, i.e., 250 μg/mouse at 24 h and 125 μg/mouse at 48 h post-PPE treatment. The intratracheal administration of L4 was also attempted. Administration of 1, 0.3, or 0.1 mg of L4 per mouse (1 mg, unless otherwise specified) occurred 1 day before the PPE treatment (4 U). Bronchoalveolar lavage (BAL) fluid was collected using the same procedure that was used for intravenous administration. xxxMicro-computer tomography assessment was included to analyze the destruction of alveolar compartments, as reported previously (18).

Dexamethasone administration. Mice were administered 1 mg of L4 or 3.9 mg/kg of dexamethasone (DEX) sodium phosphate (Solcort; Fujipharma, Tokyo, Japan), corresponding to 3 mg/kg as dexamethasone, according to manufacturer's instructions, was administered 1 day after the LPS treatment. Seven days later, BAL fluid was collected for analysis using the same procedure as that used in the case of intravenous administration.

Migration assay. Neutrophils from mouse bone marrow were purified using a discontinuous Percoll gradient, as described previously (3). Cells were then washed and resuspended in Hanks' balanced salt solution. Cells were first treated with 1 mg/ml of L4 or PBS at 37°C for 30 min. A total of 1×10^6 cells were placed on a 3-μm-pore size membrane of cell culture inserts (Merck-Millipore), and the lower well of the migration plate contained 500 μl of medium with or without 1×10^{-5} M *N*-formyl-methionyl-leucyl-phenylalanine (fMLP) (Sigma-Aldrich). The 24-well migration plate was incubated at 37°C for 90 min in a 5% CO_2 humidified atmosphere. After incubation, the filter was stained with Diff-Quik (International Reagents, Kobe, Japan), and the number of migrated cells on the undersurface of the filter was counted in five random high-power fields (×400). Experiments were performed in triplicate.

BAL fluid analysis. BAL fluid was retrieved via a 22-gauge intravenous catheter inserted into the trachea of mice. Total cell counts of the BAL fluid were determined with a hemocytometer after the destruction of red blood cells. Cell subsets in the BAL fluid were examined by cytospin preparation staining with Hema3 (Biochemical Sciences, Swedesboro, NJ) or Diff-Quik reagent (Sysmex Interna-

tional Reagents, Kobe, Japan). Differential counts were performed by examining >300 cells with a standard light microscope. Myeloperoxidase (MPO) activity in BAL fluid was measured as described previously (21).

ELISA for cytokines. Cytokines (IL-6 and TNF-α) in BAL (at *day 1* shown in Fig. 2*C*) were quantified using a Mouse IL-6 ELISA Ready-SET-Go! (eBioscience, San Diego, CA) and Mouse TNF-α ELISA Ready-SET-Go! (eBioscience), respectively, according to the manufacturer's protocol.

L4 quantification in BAL and blood. BAL or plasma was diluted with water and then boiled for 5 min. After an equal volume of phenol-chloroform was added and followed with being vortexed for 30 s, the samples were centrifuged at 20,000 *g* for 15 min at room temperature. The supernatant was transferred to Amicon Ultra-0.5 ml 10K (Merck Millipore) and then centrifuged at 14,000 *g* for 30 min at 4°C. After filtration (0.22 μm), the samples were injected into HPLC (Prominence; Shimadzu, Kyoto, Japan). Separation of L4 in reverse-phase HPLC and postcolumn fluorescent labeling with cyanoacetamide was performed according to a previous report (29) with modifications. Unison UK-Amino 150 × 4.6 mm column (Imtakt, Kyoto, Japan) was used for this separation. The HPLC eluents used were A, 2.5% ethanol; B, 2.5% ethanol, 800 mM Na_2SO_4. The gradient program (flow rate: 0.4 ml/min) was 0–30 min, 0–25% eluent B; 30–40 min, 50% eluent B. 2-Cyanoacetamide (2%) in 50 mM $Na_2B_4O_7$, pH 9.7, was added to the effluent at 0.225 ml/min, and the mixture was passed through a dry reaction bath (DB-5; Shimamura Instrument, Tokyo, Japan) at 145°C for 5 min. Fluorescence (ex/em, 331/383 nm) of the labeled L4 was detected.

Zymography. Mouse BAL fluid was assessed by gelatin zymography. To semi-quantify gelatinolytic activities, gel images were captured using a Scan Jet II cx/T (Hewlett-Packard, Palo Alto, CA), and band intensities were calculated using National Institutes of Health Image software (Image J, version 1.54, ML), as described previously (22). Relative intensities of zymography were expressed as arbitrary units (AU).

Quenched fluorescent assay against generic MMP activity. Culture supernatants of RAW 264.7 cells were used as an enzyme source. The altered total MMP activity was examined directly by cleavage of the quenched fluorescent substrate Dnp-Pro-b-cyclohexyl-Ala-Gly-Cys(Me)-His-Ala-Lys(N-Me-2-aminobenzoyl)-NH_2 (Calbiochem, San Diego, CA), with various types of sugars. The culture supernatant was desalted using centrifugal filter devices with regenerated cellulose 30,000 MWCO (Merck-Millipore) beforehand. Fluorescent substrate (4 μM) was added to initiate the enzymatic reaction, following a preincubation of sugars and culture supernatant at 37°C for 1 h. Fluorescence intensity was measured at 495 nm (excitation) and 520 nm (emission) at 5-min intervals for the entire reaction period. Data were plotted as fluorescence intensity versus time for each sample. Initial rates, used to evaluate the MMP inhibitory effect of sugars, were calculated over a time period, typically 20 min, where the cleavage of substrate was linear with respect to time and did not exceed 10% conversion. All of the experiments were performed in triplicate.

Microcomputer tomography assessment of emphysema. PPE-treated mice or corresponding control mice were scanned by microcomputer tomography (micro-CT), and density histograms were created from all the transaxial micro-CT images (Hitachi Aloka Medical, Mitaka, Japan) within the lung fields, as described previously (18). Low-attenuation area (LAA) thresholds were set in the range ~871 to ~610 Hounsfield units, and LAA% was calculated using the ratio of the LAA volume to the total lung volume. The LAA% was used to assess the progress of alveolar destruction.

Data presentation and statistical analysis. Data are expressed as the means ± SE unless otherwise indicated, and the Student's *t*-test was used to compare two groups. The Tukey-Kramer method and the Tukey method using the StatView J 5.0 System software (SAS Institute, Cary, NC) were used to compare three or more groups. Statistical significance was set at $P < 0.05$ and $P < 0.01$.

RESULTS

KS levels in lungs are diminished in mice exposed to cigarette smoke. KS is the most abundant GAG present in the airway mucus, and cells in the surface epithelium are responsible for the synthesis and release of KS or KS-like molecules into airway secretions. To study the biological function of KS in lung injuries, we examined its expression in mouse lung by using an anti-KS (5D4) antibody. We examined KS levels in normal and 3-mo smoke-exposed mouse lungs. Histological sections of lungs stained with the anti-KS antibody and with a marker for type I (aquaporin-5) or type II (surfactant protein-C) pneumocytes showed that KS (shown in red) is expressed in endothelial cells (Fig. 1*A*), immune cells (Fig. 1, *B* and *C*), and in fibroblasts (Fig. 1*D*), but not in lung epithelial cells (shown in green). After a 3-mo smoke exposure, although signals in endothelial cells partially remained in some areas (Fig. 1*E*), KS

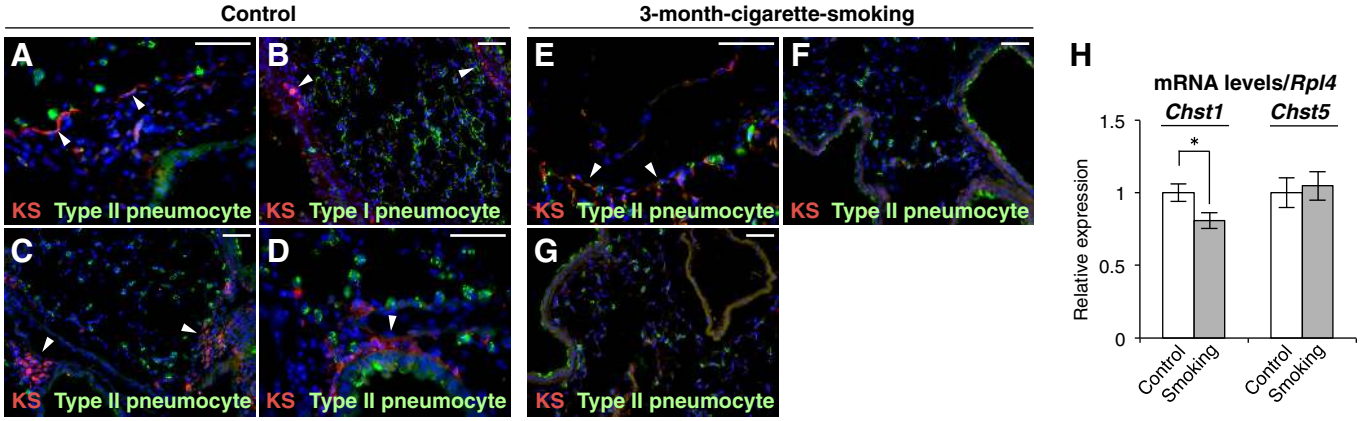

Fig. 1. Keratan sulfate (KS) is decreased by cigarette smoking. *A–G*: histological sections of murine lungs were fluorescently stained for KS using anti-KS (5D4) antibody (red), surfactant protein-C (a marker for type II pneumocyte) (*A*, *C–G*; green) or aquaporin-5 (a marker for type I pneumocyte) (*B*; green), and for nuclei using DAPI (blue). 5D4 reactivity was observed in endothelial cells (*A*, *E*), immune cells (*B*, *C*), and fibroblasts (*D*), as indicated by arrowheads. Scale bar: 50 μm. *H*: mRNA levels of *Chst1* and *Chst5* genes relative to that of *Rpl4* in lung from control or 3-mo smoke-exposed mice were quantified ($n = 6$). *Chst2* mRNA encoding another sulfotransferase for KS was undetectable in mouse lung. All graphs show means ± SE, and statistical analyses were performed using Student's *t*-test. *$P < 0.05$.

expression in the lung was largely reduced (Fig. 1, *F* and *G*). To further examine the issue of whether KS expression is altered by smoking, we focused on the three KS sulfotransferases: KSGal6ST, encoded by *Chst1* (5); GlcNAc6ST-1, encoded by *Chst2* (34); and GlcNAc6ST-3, encoded by *Chst5* (1), which are responsible for KS biosynthesis. Real-time PCR analyses found that mRNA level of *Chst1* in mouse lungs were decreased by cigarette-smoking (*Chst2* being undetectable) (Fig. 1*H*), further indicating that KS expression is downregulated by smoking. These findings suggest that the decreased level of KS may be related to lung injury and that lung KS may have a protective function under normal physiological conditions.

L4 treatment attenuates early lung inflammation in a PPE-induced emphysema mouse model. We next investigated the effect of L4 on neutrophil migration, because neutrophil influx is implicated in lung inflammation and the development of COPD (10, 26). Neutrophils were isolated from mouse bone marrow tissue and subjected to a chemotaxis assay. There were six times as many cells as controls that migrated to the lower wells containing the chemoattractant fMLP, and cells that were pretreated with 1 mg/ml L4 demonstrated a 50% decrease in migration (Fig. 2, *A* and *B*). This suggests that L4 has the capacity to suppress neutrophil-mediated inflammation. On the basis of these findings, we tested L4 in an elastase-induced emphysema mouse model (Fig. 2*C*). An analysis of BAL fluid indicated that an intravenous L4 pretreatment resulted in a significant decrease in the influx of inflammatory cells, especially neutrophils and macrophages (Fig. 2*D*) and that this effect was L4-dose-dependent (Fig. 2*E*). In accordance with the decrease of neutrophils in BAL fluid, activity of antimicrobial enzyme MPO in BAL, which is induced by a 24-h period of PPE administration, was significantly decreased by L4 pretreatment (Fig. 2*F*). We also confirmed the reduction in inflammatory cytokines (IL-6 and TNF-α) in BAL (Fig. 2*G*). These data suggest that L4 blocks both immune cell migration and subsequent inflammation in the lung.

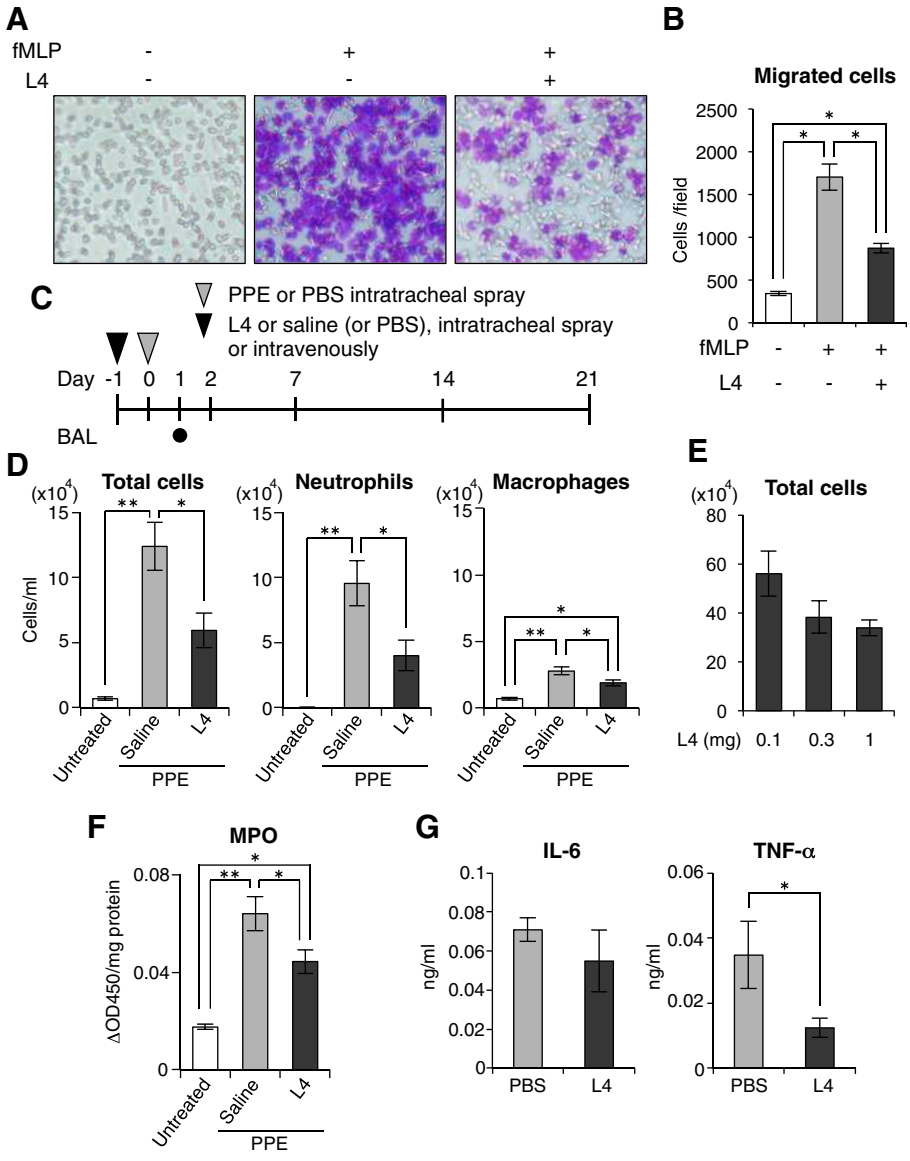

Fig. 2. L4 ([SO_3^--6]Galβ1–4[SO_3^--6]GlcNAc) treatment inhibits inflammatory outcomes in elastase-induced acute lung inflammation. *A*: chemotaxis of purified neutrophils was determined. Cells that had migrated to the lower surface of the membrane were fixed and stained with Diff-Quik. Representative fields of cell migration were photographed using a phase-contrast microscope. The purple color indicates cells that had migrated. *B*: numbers of migrated cells were quantified (n = 3). *C*: protocols for the treatment of animals. L4 was administered intratracheally (*E*, *G*) or intravenously (*D*, *F*). *D*: after the administration of L4 and porcine pancreatic elastase (PPE), the numbers of total cells, neutrophils, and macrophages in bronchoalveolar lavage (BAL) fluid were determined (n = 5, 13, 16 for untreated, saline pretreatment, and L4 pretreatment, respectively). *E*: total cell numbers in BAL fluid (n = 6), after the administration of PPE and various doses of L4 (intratracheal). *F*: MPO activity in BAL was measured (n = 5, 13, 16 for untreated, saline pretreatment, and L4 pretreatment, respectively). *G*: levels of IL-6 and TNF-α in BAL (n = 7, 11 for PBS and L4 treatment, respectively). All graphs show means ± SE, and statistical analyses were performed using the Tukey-Kramer method for multiple comparisons or Student's t-test for two groups. $^*P < 0.05$ and $^{**}P < 0.01$.

To confirm that intratracheally administered L4 reaches alveoli, we quantified the L4 levels in mouse BAL and plasma after an L4 administration. We established a quantification method for L4 using HPLC, in which exogenously L4 was added to untreated mouse plasma or BAL, which was recovered with good linearity (Fig. 3*A*). By using this method, after intratracheal administration, L4 was detected in BAL fluid (Fig. 3*B*) and, subsequently, in plasma (Fig. 3*C*) with a half-life of 45 and 129 min, respectively, showing that intratracheally administered L4 does, in fact, reach alveoli.

L4 treatment decreases MMP-2 and MMP-9 in BAL fluid in a PPE-induced emphysema mouse model. We also examined whether L4 had an inhibitory effect on MMP production or activity in the lung. Activity of MMP-2 and MMP-9 in BAL fluid from elastase-induced emphysema model mice were analyzed by gelatin zymography. In this model, both MMP-2 and MMP-9 levels were significantly elevated in BAL fluid at 24 h after PPE administration, and we found that an L4 pretreatment decreased the gelatinolytic activities of MMP-2 and MMP-9 in BAL fluid (Fig. 4, *A* and *B*). Moreover, a quenched fluorescence assay for MMP-9 activity was done on BAL fluid. The level of MMP-9 activities in the L4-pretreated mice was only one-third that for the PBS-treated mice (Fig. 4*C*). Similar results were obtained using culture medium from a mouse macrophage cell line, RAW 264.7, as an enzyme source of MMP. Treatment with 1 mg/ml solution of L4 reduced generic MMP activity to ~70% of the control (Fig. 4*D*). Although a commercial MMP inhibitor, GM6001 (25 μM), showed a stronger inhibition on MMP activity, other disaccharides LacNAc and lactose did not inhibit MMP activity.

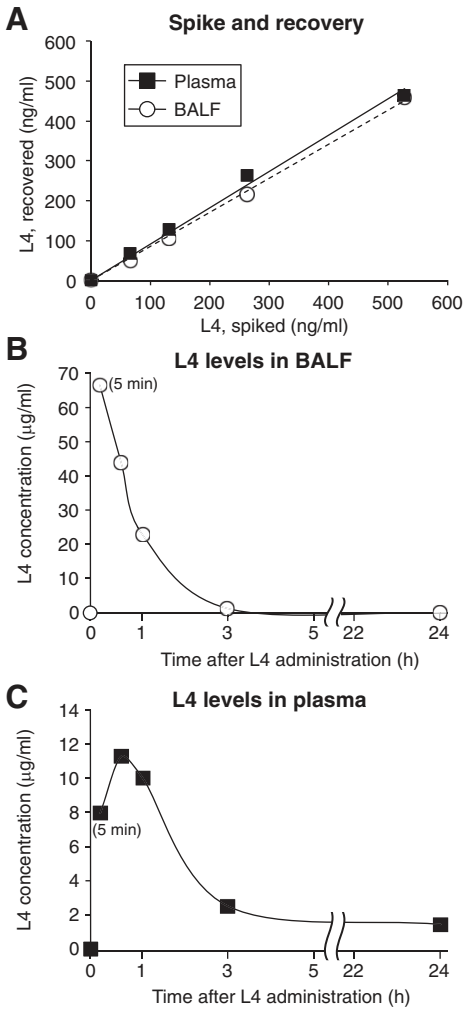

Fig. 3. Detection of L4 in BAL fluid and plasma after intratracheal administration. *A*: L4 was exogenously added to untreated mouse plasma or BAL fluid at various concentrations, and L4 levels were then quantified by postcolumn fluorescence labeling and detection using HPLC. *B* and *C*: L4 (1 mg/mouse) was intratracheally administered, and then L4 levels were quantified in BAL (*B*) and plasma (*C*), which were collected at different time points (5 min, 30 min, 1 h, 3 h, and 24 h). Data from unadministered mice were plotted at *time 0*.

L4 treatment reduces the PPE-induced enlargement of air space in mice. We next examined the therapeutic effect of L4 on lung destruction. Histochemical analyses of lung tissue were performed on *day 14* or *21* after the intratracheal administration of PPE (Fig. 5*A*). Examination of histological sections showed that PPE induced a significant enlargement of the air space due to the destruction of alveolar walls. The use of the L_m as a measure of the average distance between alveolar walls provides an indication of the severity of emphysema. This value was significantly reduced in animals that had been pretreated intravenously with L4 (72 ± 3.8 vs. 86 ± 3.5 μm in saline-treated mice) (Fig. 5*B*).

We next administered L4 intratracheally, a much more direct method of delivery (Fig. 5*C*), and, therefore, much easier for patients to receive if this therapy were applied clinically. The progression of emphysema was evaluated using micro-CT, which allows a quantitative assessment to be made in living mice and humans (7). Reconstructed three-dimensional structure images of the murine lung (*day 21*) clearly showed that the area of emphysema (shown in yellow) was reduced as the result of the L4 pretreatment (Fig. 5*D*, *left*). LAA % was calculated as the ratio of LAA to the total lung area. We found a significant decrease in LAA % in the L4-pretreated mice at *days 7*, *14*, and *21* (Fig. 5*D*, *right*). These data show that L4 was effective in reducing alveolar destruction in the PPE-induced lung injury.

L4 treatment is as effective as dexamethasone in inhibiting LPS-induced inflammation in cigarette smoke-exposed mice. We finally evaluated whether or not L4 also inhibits LPS-induced inflammation. For this purpose, we used *Fut8*-heterozygous ($Fut8^{+/-}$) mice, which were previously found to develop emphysema easily after a 3-mo period of exposure to cigarette smoke (8). After an LPS treatment to cigarette smoke-exposed mice, L4 (1 mg/mouse, intratracheally) or DEX (intravenously) was administered, and BAL fluid was collected and assayed on *day 7*, as shown in Fig. 6*A*. L4 reduced the accumulation of inflammatory cells, including macrophages and neutrophils, in the alveolar space to about half of that in mice that had been treated with saline only. Moreover, the effect of L4 was nearly the same as that of DEX (Fig. 6*B*), an anti-inflammatory agent that is widely used to treat COPD patients with exacerbations.

DISCUSSION

Since an inflammatory event is one of the most important factors triggering the onset and/or progression of COPD (12), a clear understanding of changes in lung GAGs and of their pathological significance represents a potentially novel ap-

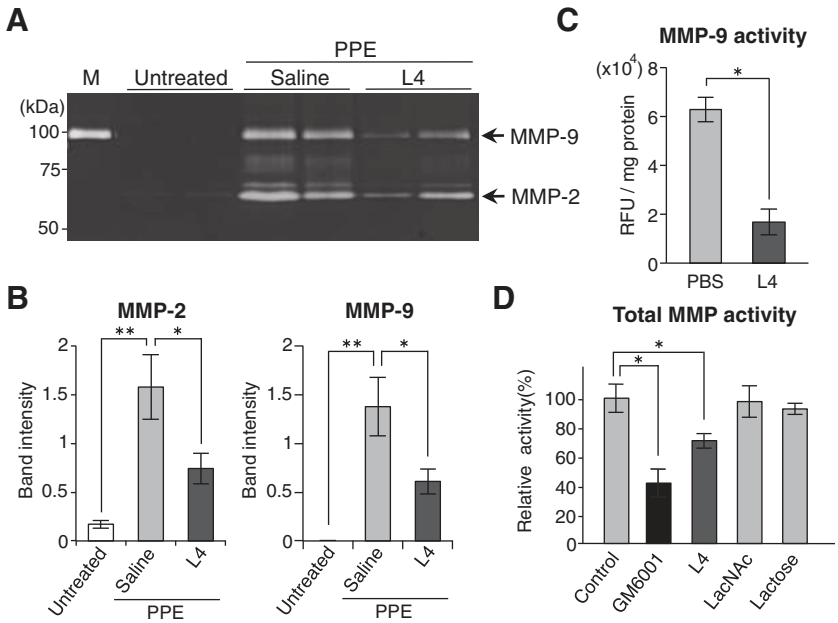

Fig. 4. L4 treatment decreases matrix metalloproteinase (MMP)-2 and MMP-9 activity in BAL. Mice were divided into three groups as in the case of Fig. 2, *D* and *F*: PPE-untreated or PPE-treated group with pretreatment of saline or L4. *A*: gelatin zymography was performed on BAL fluid collected from all of the mice at 24 h after PPE administration. *B*: band intensity of MMP-2 and MMP-9 were semiquantified ($n = 5$, 13, 16 for untreated, saline pretreatment, and L4 pretreatment, respectively). *C*: MMP-9 enzyme activity in BAL fluid was measured using SensoLyte 520 MMP-9 fluorimetric assay kit (Anaspec, Freemont, CA) ($n = 5$). *D*: total MMP activities from culture media of RAW 264.7 cells. In addition to L4, other oligosaccharides (LacNAc and lactose) were used as negative controls. GM6001, an MMP inhibitor, was used as a positive control. The MMP activities relative to that of untreated cell culture medium are shown ($n = 3$). All graphs are means ± SE, and statistical analyses were performed using the Tukey-Kramer method for multiple comparisons or Student's *t*-test for two groups. $^*P < 0.05$ and $^{**}P < 0.01$.

proach to the design of therapeutic strategies for the treatment of COPD.

A reduction in KS frequently occurs in association with inflammation (14). The biosynthesis of KS is a complicated process, which includes two kinds of enzymes: glycosyl- and sulfo-transferases (6). We found that a KS sulfotransferase (*Chst1* encoding KSGal6ST) was downregulated in mouse lung by cigarette smoking (Fig. 1*H*), but the possibility that other mechanisms are also involved in the reduction of KS cannot be excluded. As KS is typically not found to be a free

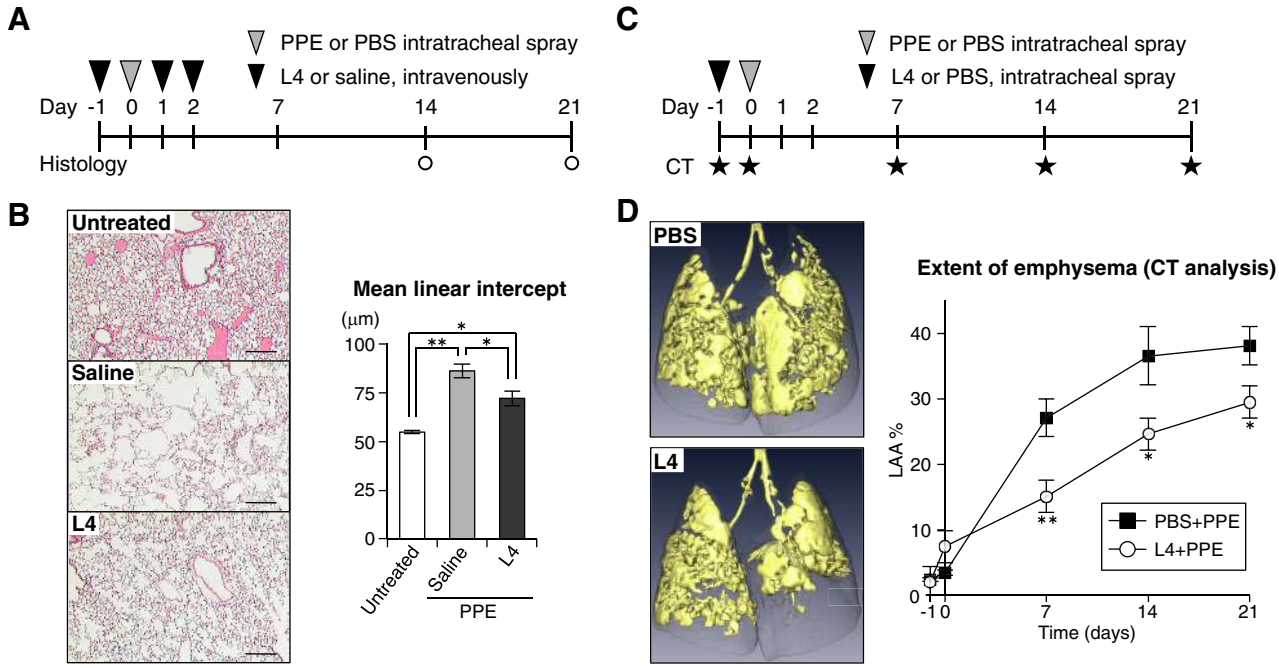

Fig. 5. L4 treatment attenuates PPE-induced alveolar damage. *A*: mice were treated intravenously with saline or L4 three times. *B*: hematoxylin and eosin-stained sections were used for morphological analyses. Representative images of lungs from PPE-untreated, saline pretreatment, or L4 pretreatment groups on *day 21* after PPE administration are shown (*left*). Original magnification is ×200. Scale bar: 200 μm. Mean linear intercepts (L_m) of alveoli on *day 21* is shown (*right*) ($n = 5$, 9, and 9 for untreated, saline-pretreated, and L4-pretreated groups, respectively). *C*: mice were treated intratracheally with PBS or L4 (1 mg/mouse) at 24 h before intratracheal PPE (4 U/mouse) inhalation. The progress of the emphysema was then monitored by micro-computer tomography (micro-CT). *D*: three-dimensional lung images (*day 21*) in which the low attenuation area (LAA) is shown in yellow, and the whole lung field is shown as a transparent shape (*left*). *Top*: PBS treatment. *Bottom*: L4 treatment. LAA % measured by micro-CT analysis was compared between PBS- and L4-pretreated groups on *days 0*, *7*, *14*, and 21 after PPE administration (*right*) ($n = 5$ and 6 for PBS-pretreated and L4-pretreated, respectively). Statistical tests were performed between the PBS and L4 groups at each time point. All graphs are means ± SE, and statistical analyses were performed using the Tukey-Kramer method for multiple comparisons or Student's *t*-test for two groups. $^*P < 0.05$ and $^{**}P < 0.01$.

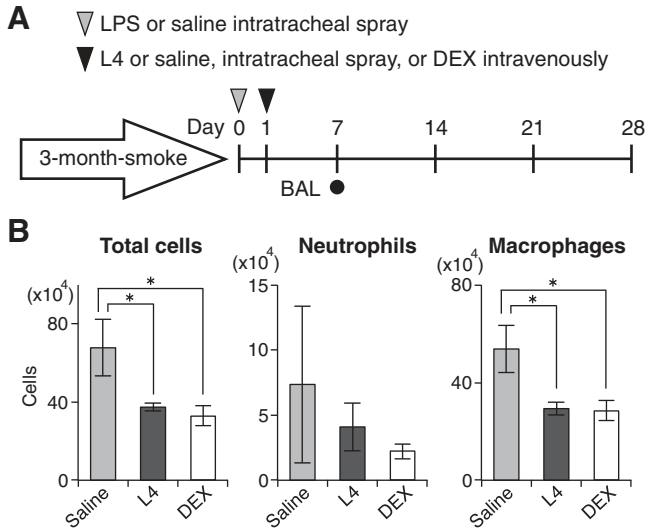

Fig. 6. L4 shows an anti-inflammatory effect in LPS-induced chronic obstructive pulmonary disease (COPD) exacerbation model mice. *A*: emphysema was induced by 3 mo exposure of *Fut8*$^{+/-}$ mice to cigarette smoke, and LPS (1 mg/kg) was then administered to induce an exacerbation event in these animals. L4 (1 mg/mouse) or saline was administered intratracheally one day later. *B*: evaluation of inflammatory cell accumulation. Data are expressed as means ± SE (n = 6, 7, and 6 for saline-, L4-, and dexamethazone (DEX)-treated groups, respectively). *$P < 0.05$ compared with saline treatment group as measured by one-way ANOVA with Tukey's post hoc test.

GAG, most of its biological functions are considered to be associated with KS proteoglycans, such as lumican and related structures in the human lung (4). Therefore, inflammation-induced KS-linked protein degradation may be partly responsible for the reduction in KS. Although the reasons why KS levels are diminished by cigarette smoke are not completely clear at present, the KS reduction is an important factor in plotting a course for creating a glycan-based therapeutics for lung disease.

L4 was found to be effective in attenuating the inflammation processes in mice in the present study (Fig. 2). By suppressing excessive immune responses, the L4 treatment exerted protective effects against alveolar inflammation, as well as alveolar destruction. Although anti-inflammatory corticosteroids are widely used for persistent or acute exacerbations of COPD patients, the worse outcomes and adverse effects of corticosteroid treatment have been reported (17). It is noteworthy that L4 has similar efficacy to that of dexamethazone, as shown in Fig. 6, suggesting that the L4 would be an effective therapy for the steroid-resistant COPD patients (15).

MMP-2 and MMP-9 activities were reduced in BAL fluid as the result of L4 administration, although the mechanism by which MMP activities are downregulated is unclear. It is possible that the decreased numbers of inflammatory cells partly contribute to this. On the other hand, as lumican has been shown to inhibit MMP-14 activity (25), there is an undeniable possibility that there is a direct interaction between KS and MMPs. An earlier report on the chondroitin sulfate proteoglycan (20) indicated that GAGs regulate the activity of MMPs at extracellular sites, where substrate degradation and matrix remodeling occur. It was suggested that the specificity of protein–GAG interactions is governed by ionic attractions between sulfate and carboxylate groups of GAGs, with the basic amino acids on the protein, as well as the optimal structural fit of the GAG chain into the binding site of the protein (31).

L4 is indicated to significantly reduce fMLP-mediated neutrophil migration. In contrast, L4 did not directly inhibit the production of reactive oxygen species or MPO activity in neutrophils in vitro (Ota F Kizuka Y, Taniguchi N, unpublished results). Considering these results, one of anti-inflammatory actions of L4 likely involves the blockade of neutrophil migration. As the exposure of neutrophils to fMLP induced an immediate polarization, which resulted in directional migration, preincubation of L4 may interfere with this process via reducing phosphorylation and surface distribution of membrane proteins, or decreasing the activation of MAP kinases of neutrophil. Determining how L4 blocks neutrophil migration and how L4 suppresses inflammation in vivo is an important focus of our next project.

Although the concentration of L4 used in this study was ~250 μg/mouse, which is ~4 mM, no adverse effects were found in vivo and in vitro. Our data showed that the half-life of L4 is ~129 min in blood (Fig. 3*C*) and that one to three injections of L4 in the experimental model mice were found to be effective. Attempts to identify more stable, longer-acting, lower-dose L4 derivatives will provide a significant challenge for future studies, and suitable protocols for the dosage and frequency of L4 administration are required to establish more effective treatments for COPD exacerbations.

During the progress of COPD, cigarette smoking, viruses and bacteria, and air pollutants will induce inflammation and MMP production from various lung cells (e.g., neutrophils, macrophages, and lung epithelial cells). We showed that L4 suppresses both directly and indirectly the MMP enzyme activity (Fig. 4), which may play an important role in alveolar destruction. More importantly, L4 reduced the influx of inflammatory cells and the subsequent production of cytokines and MPO, and directly inhibited neutrophil migration. This might be due to interference with the polarization of neutrophils (e.g., the expression pattern of β2-integrin). As MPO was suggested to have a proinflammatory cytokine-like function (19), the reduction in MPO activity could partially contribute to the anti-inflammatory action of L4. Moreover, we previously reported that L4 has inhibitory activity on flagellin-induced IL-8 production, which is known to be chemoattractant of inflammatory cells. Therefore, it appears that L4 functions to attenuate emphysema through its multiple anti-inflammatory activ-

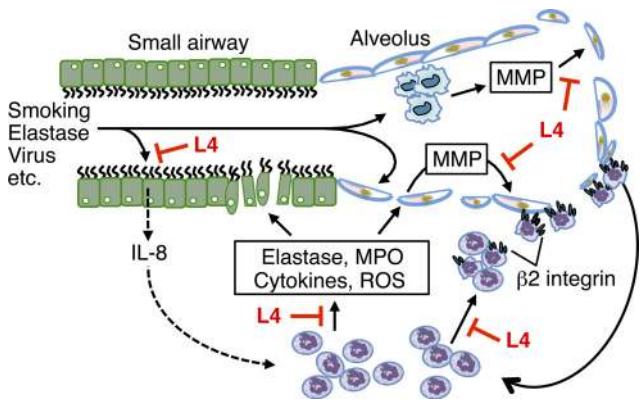

Fig. 7. Amelioration of COPD pathology by multiple anti-inflammatory actions of L4.

ities (Fig. 7). Our next important challenge will be to identify a direct target protein (receptor) of L4, which can mediate glycan-targeted COPD therapy.

ACKNOWLEDGMENTS

The authors thank Emmanuel Siota Palacpac for technical assistance for Conxiao Gao and Kazuaki Ohtsubo. The authors also thank Dr. Milton Feather for help with the English editing, and Dr. Kenji Uchimura and Dr. Gabriel Rabinovich for valuable comments and criticism of our work.

GRANTS

This work was partly supported by the Program for Promotion of Fundamental Studies in Health Science of the National Institute of Biomedical Innovation, The Japan Society for the Promotion of Science (Grant-in-Aid for Challenging Exploratory Research to N. Taniguchi (Grant 15K14481), a Grant-in-Aid for Scientific Research (B) to N. Taniguchi (Grant 15H04700), and the program for the RIKEN-Max Planck joint research. P. H. Seeberger, C. Rademacher and J. Aretz are generously supported by the Max Planck Society. C. Rademacher acknowledges the support of the German Research Foundation (DFG, Emmy Noether Program, RA1944/2–1), and the Chemical Industry Foundation. B. Lepenies acknowledges funding from the German Federal Ministry of Education and Research, and the Collaborative Research Center.

DISCLOSURES

No conflicts of interest, financial or otherwise, are declared by the authors.

AUTHOR CONTRIBUTIONS

C.G., R.F., T.Y., M.U., F.O., T.H., H. Korekane, B.L., J.A., C.R., H. Kabata, and A.E.H. performed experiments; C.G., R.F., T.Y., M.U., Y.K., and A.E.H. analyzed data; C.G., T.Y., M.U., Y.K., S.K., T.M., K.O., K.Y., Y.Y., B.L., A.E.H., P.H.S., T.B., K.K., and N.T. interpreted results of experiments; C.G., R.F., and Y.K. prepared figures; C.G., T.B., and N.T. drafted manuscript; C.G., R.F., T.Y., M.U., F.O., Y.K., T.H., H. Korekane, S.K., T.M., K.O., K.Y., Y.Y., B.L., J.A., C.R., H. Kabata, A.E.H., P.H.S., T.B., K.K., and N.T. edited and revised manuscript; C.G., R.F., T.Y., M.U., F.O., Y.K., T.H., H. Korekane, S.K., T.M., K.O., K.Y., Y.Y., B.L., J.A., C.R., H. Kabata, A.E.H., P.H.S., T.B., K.K., and N.T. approved final version of manuscript.

REFERENCES

1. **Akama TO, Misra AK, Hindsgaul O, Fukuda MN.** Enzymatic synthesis in vitro of the disulfated disaccharide unit of corneal keratan sulfate. *J Biol Chem* 277: 42,505–42,513, 2002. doi:10.1074/jbc.M207412200.
2. **Barnes PJ.** Alveolar macrophages in chronic obstructive pulmonary disease (COPD). *Cell Mol Biol (Noisy-le-grand)* 50: OL627–OL637, 2004.
3. **Boxio R, Bossenmeyer-Pourié C, Steinckwich N, Dournon C, Nüsse O.** Mouse bone marrow contains large numbers of functionally competent neutrophils. *J Leukoc Biol* 75: 604–611, 2004. doi:10.1189/jlb.0703340.
4. **Dolhnikoff M, Morin J, Roughley PJ, Ludwig MS.** Expression of lumican in human lungs. *Am J Respir Cell Mol Biol* 19: 582–587, 1998. doi:10.1165/ajrcmb.19.4.2979.
5. **Fukuta M, Inazawa J, Torii T, Tsuzuki K, Shimada E, Habuchi O.** Molecular cloning and characterization of human keratan sulfate Gal-6-sulfotransferase. *J Biol Chem* 272: 32,321–32,328, 1997. doi:10.1074/jbc.272.51.32321.
6. **Funderburgh JL.** Keratan sulfate biosynthesis. *IUBMB Life* 54: 187–194, 2002. doi:10.1080/15216540214932.
7. **Galbán CJ, Han MK, Boes JL, Chughtai KA, Meyer CR, Johnson TD, Galbán S, Rehemtulla A, Kazerooni EA, Martinez FJ, Ross BD.** Computed tomography-based biomarker provides unique signature for diagnosis of COPD phenotypes and disease progression. *Nat Med* 18: 1711–1715, 2012. doi:10.1038/nm.2971.
8. **Gao C, Maeno T, Ota F, Ueno M, Korekane H, Takamatsu S, Shirato K, Matsumoto A, Kobayashi S, Yoshida K, Kitazume S, Ohtsubo K, Betsuyaku T, Taniguchi N.** Sensitivity of heterozygous $\alpha_{1,6}$-fucosyltransferase knock-out mice to cigarette smoke-induced emphysema: implication of aberrant transforming growth factor-β signaling and matrix metalloproteinase gene expression. *J Biol Chem* 287: 16699–16708, 2012. doi:10.1074/jbc.M111.315333.
9. **Hegab AE, Arai D, Gao J, Kuroda A, Yasuda H, Ishii M, Naoki K, Soejima K, Betsuyaku T.** Mimicking the niche of lung epithelial stem cells and characterization of several effectors of their in vitro behavior. *Stem Cell Res (Amst)* 15: 109–121, 2015. doi:10.1016/j.scr.2015.05.005.
10. **Hoenderdos K, Condliffe A.** The neutrophil in chronic obstructive pulmonary disease. *Am J Respir Cell Mol Biol* 48: 531–539, 2013. doi:10.1165/rcmb.2012-0492TR.
11. **Hogg JCCF, Chu F, Utokaparch S, Woods R, Elliott WM, Buzatu L, Cherniack RM, Rogers RM, Sciurba FC, Coxson HO, Paré PD.** The nature of small-airway obstruction in chronic obstructive pulmonary disease. *N Engl J Med* 350: 2645–2653, 2004. doi:10.1056/NEJMoa032158.
12. **Holloway RA, Donnelly LE.** Immunopathogenesis of chronic obstructive pulmonary disease. *Curr Opin Pulm Med* 19: 95–102, 2013. doi:10.1097/MCP.0b013e32835cfff5.
13. **Isnard N, Robert L, Renard G.** Effect of sulfated GAGs on the expression and activation of MMP-2 and MMP-9 in corneal and dermal explant cultures. *Cell Biol Int* 27: 779–784, 2003. doi:10.1016/S1065-6995(03)00167-7.
14. **Jander S, Schroeter M, Fischer J, Stoll G.** Differential regulation of microglial keratan sulfate immunoreactivity by proinflammatory cytokines and colony-stimulating factors. *Glia* 30: 401–410, 2000. doi:10.1002/(SICI)1098-1136(200006)30:4<401::AID-GLIA90>3.0.CO;2-6.
15. **Jiang Z, Zhu L.** Update on molecular mechanisms of corticosteroid resistance in chronic obstructive pulmonary disease. *Pulm Pharmacol Ther* 37: 1–8, 2016. doi:10.1016/j.pupt.2016.01.002.
16. **Kamio K, Yoshida T, Gao C, Ishii T, Ota F, Motegi T, Kobayashi S, Fujinawa R, Ohtsubo K, Kitazume S, Angata T, Azuma A, Gemma A, Nishimura M, Betsuyaku T, Kida K, Taniguchi N.** $\alpha_{1,6}$-Fucosyltransferase (Fut8) is implicated in vulnerability to elastase-induced emphysema in mice and a possible non-invasive predictive marker for disease progression and exacerbations in chronic obstructive pulmonary disease (COPD). *Biochem Biophys Res Commun* 424: 112–117, 2012. doi:10.1016/j.bbrc.2012.06.081.
17. **Kiser TH, Allen RR, Valuck RJ, Moss M, Vandivier RW.** Outcomes associated with corticosteroid dosage in critically ill patients with acute exacerbations of chronic obstructive pulmonary disease. *Am J Respir Crit Care Med* 189: 1052–1064, 2014. doi:10.1164/rccm.201401-0058OC.
18. **Kobayashi S, Fujinawa R, Ota F, Kobayashi S, Angata T, Ueno M, Maeno T, Kitazume S, Yoshida K, Ishii T, Gao C, Ohtsubo K, Yamaguchi Y, Betsuyaku T, Kida K, Taniguchi N.** A single dose of lipopolysaccharide into mice with emphysema mimics human chronic obstructive pulmonary disease exacerbation as assessed by micro-computed tomography. *Am J Respir Cell Mol Biol* 49: 971–977, 2013. doi:10.1165/rcmb.2013-0074OC.
19. **Lau D, Mollnau H, Eiserich JP, Freeman BA, Daiber A, Gehling UM, Brümmer J, Rudolph V, Münzel T, Heitzer T, Meinertz T, Baldus S.** Myeloperoxidase mediates neutrophil activation by association with CD11b/CD18 integrins. *Proc Natl Acad Sci USA* 102: 431–436, 2005. doi:10.1073/pnas.0405193102.
20. **Monzon MEC-MS, Casalino-Matsuda SM, Forteza RM.** Identification of glycosaminoglycans in human airway secretions. *Am J Respir Cell Mol Biol* 34: 135–141, 2006. doi:10.1165/rcmb.2005-0256OC.
21. **Moriyama C, Betsuyaku T, Ito Y, Hamamura I, Hata J, Takahashi H, Nasuhara Y, Nishimura M.** Aging enhances susceptibility to cigarette smoke-induced inflammation through bronchiolar chemokines. *Am J Respir Cell Mol Biol* 42: 304–311, 2010. doi:10.1165/rcmb.2009-0025OC.
22. **Odajima N, Betsuyaku T, Nasuhara Y, Inoue H, Seyama K, Nishimura M.** Matrix metalloproteinases in blood from patients with LAM. *Respir Med* 103: 124–129, 2009. doi:10.1016/j.rmed.2008.07.017.
23. **Pauwels RA, Buist AS, Calverley PM, Jenkins CR, Hurd SS, GOLD Scientific Committee.** Global strategy for the diagnosis, management, and prevention of chronic obstructive pulmonary disease. NHLBI/WHO Global Initiative for Chronic Obstructive Lung Disease (GOLD) Workshop summary. *Am J Respir Crit Care Med* 163: 1256–1276, 2001. doi:10.1164/ajrccm.163.5.2101039.
24. **Pauwels RAR, Rabe KF.** Burden and clinical features of chronic obstructive pulmonary disease (COPD). *Lancet* 364: 613–620, 2004. doi:10.1016/S0140-6736(04)16855-4.
25. **Pietraszek K, Chatron-Colliet A, Brézillon S, Perreau C, Jakubiak-Augustyn A, Krotkiewski H, Maquart FX, Wegrowski Y.** Lumican: a new inhibitor of matrix metalloproteinase-14 activity. *FEBS Lett* 588: 4319–4324, 2014. doi:10.1016/j.febslet.2014.09.040.

26. **Russell DW, Wells JM, Blalock JE.** Disease phenotyping in chronic obstructive pulmonary disease: the neutrophilic endotype. *Curr Opin Pulm Med* 22: 91–99, 2016. doi:10.1097/MCP.0000000000000238.
27. **Shirato K, Gao C, Ota F, Angata T, Shogomori H, Ohtsubo K, Yoshida K, Lepenies B, Taniguchi N.** Flagellin/Toll-like receptor 5 response was specifically attenuated by keratan sulfate disaccharide via decreased EGFR phosphorylation in normal human bronchial epithelial cells. *Biochem Biophys Res Commun* 435: 460–465, 2013. doi:10.1016/j.bbrc.2013.05.009.
28. **Suzuki M, Betsuyaku T, Ito Y, Nagai K, Odajima N, Moriyama C, Nasuhara Y, Nishimura M.** Curcumin attenuates elastase- and cigarette smoke-induced pulmonary emphysema in mice. *Am J Physiol Lung Cell Mol Physiol* 296: L614–L623, 2009. doi:10.1152/ajplung.90443.2008.
29. **Toyoda H, Kinoshita-Toyoda A, Selleck SB.** Structural analysis of glycosaminoglycans in *Drosophila* and *Caenorhabditis elegans* and demonstration that tout-velu, a *Drosophila* gene related to EXT tumor suppressors, affects heparan sulfate in vivo. *J Biol Chem* 275: 2269–2275, 2000. doi:10.1074/jbc.275.4.2269.
30. **Uozumi N, Yanagidani S, Miyoshi E, Ihara Y, Sakuma T, Gao CX, Teshima T, Fujii S, Shiba T, Taniguchi N.** Purification and cDNA cloning of porcine brain GDP-L-Fuc:*N*-acetyl-β-D-glucosaminide $\alpha_{1,6}$-fucosyltransferase. *J Biol Chem* 271: 27,810–27,817, 1996. doi:10.1074/jbc.271.44.27810.
31. **Volpi N.** Therapeutic applications of glycosaminoglycans. *Curr Med Chem* 13: 1799–1810, 2006. doi:10.2174/092986706777452470.
32. **Wang X, Inoue S, Gu J, Miyoshi E, Noda K, Li W, Mizuno-Horikawa Y, Nakano M, Asahi M, Takahashi M, Uozumi N, Ihara S, Lee SH, Ikeda Y, Yamaguchi Y, Aze Y, Tomiyama Y, Fujii J, Suzuki K, Kondo A, Shapiro SD, Lopez-Otin C, Kuwaki T, Okabe M, Honke K, Taniguchi N.** Dysregulation of TGF-β_1 receptor activation leads to abnormal lung development and emphysema-like phenotype in core fucose-deficient mice. *Proc Natl Acad Sci USA* 102: 15,791–15,796, 2005. doi:10.1073/pnas.0507375102.
33. **Xu H, Kurihara H, Ito T, Kikuchi H, Yoshida K, Yamanokuchi H, Asari A.** The keratan sulfate disaccharide Gal(6S03) $\beta_{1,4}$-GlcNAc(6S03) modulates interleukin 12 production by macrophages in murine Thy-1 type autoimmune disease. *J Biol Chem* 280: 20,879–20,886, 2005. doi:10.1074/jbc.M411954200.
34. **Zhang H, Muramatsu T, Murase A, Yuasa S, Uchimura K, Kadomatsu K.** *N*-acetylglucosamine 6-*O*-sulfotransferase-1 is required for brain keratan sulfate biosynthesis and glial scar formation after brain injury. *Glycobiology* 16: 702–710, 2006. doi:10.1093/glycob/cwj115.